Prediction of RCF Damage on Underground Metro Lines

Pelin BOYACIOGLU[1], Adam BEVAN[1] and Andy VICKERSTAFF[2]
[1].Institute of Railway Research, School of Computing and Engineering, University of Huddersfield, Huddersfield, HD1 3DH, UK
[2].London Underground, 15 Westferry Circus, Canary Wharf, E14 4HD, UK

Abstract: London Underground (LUL) is one of the largest metro networks in the world and carried nearly 1.5 billion passengers in 2015. This increasing passenger demand leads to higher axle loads and shorter headways in the railway operations. However, this has a detrimental impact on the damage generated at the wheel-rail interface. In spite of the advances in rolling stock and track engineering, new developments in material manufacturing methods and rail inspection technology, cracking in rails still remains a major concern for infrastructure managers in terms of safety and maintenance costs. In this study, field data from two metro lines on the LUL network was analysed to identify the distribution and severity of the different damage types. Detailed vehicle dynamics route simulations were conducted for the lines and the calculated wheel-rail forces were investigated to assess the applicability current models for the prediction of rail damage on metro lines. These models include the Whole Life Rail Model (WLRM), previously developed for Great Britain (GB) main line tracks, and Shakedown theory. The influence of key factors such as curve radius, different friction conditions, track irregularities and wheel-rail profiles on the wheel-rail contact interface have been evaluated and compared with outputs from simulations on mainline routes. The study found that the contact patch energy (Tγ) and the interaction between wear and RCF in rails were highly influenced by the characteristics of metro tracks. It was also shown that both the Tγ and Shakedown methods can provide successful prediction of damage susceptibility of rails. However, in order to increase the accuracy of damage predictions and to ascertain the severity of different damage types, the duty conditions which are observed by the rail and the changes in contact conditions resulting from the successive vehicle passes should be considered in the modelling.
Keywords: rolling contact fatigue, vehicle dynamics simulations, rail damage

1 Introduction

Although rolling contact fatigue (RCF) is considered to be a major factor affecting the maintainability and safety of the tracks in heavy-haul and high-speed railway lines, due to excessive axle loads and higher speeds in these routes, it is also a crucial concern for metro-underground systems. While rail damage in conventional mainline routes has been primarily investigated within previous studies (Li et al. 2008; Olofsson and Nilsson, 2002; Girsch and Heyder, 2003), there has been less emphasis placed on the development of RCF cracking in metro-underground systems. However, with the changing track characteristics, the high traffic demand as well as the reduction in the available maintenance times, means that the management of RCF cracks is also of vital importance on these lines.

In order to meet these challenges, rail damage prediction models are used to improve maintenance strategies. The wheel-rail interface team at LUL have conducted several studies to optimise their maintenance methods using damage models previously applied to main line track (Vickerstaff, 2015; 2016). The work described within this paper has been carried out in collaboration with LUL to support the further development of these models and increase the accuracy of the damage predictions for metro lines.

In this study, the Bakerloo and Jubilee lines were selected for detailed investigation. Field crack data from these lines was analysed and wheel-rail forces were calculated using detailed vehicle dynamics route simulations. The outputs from these simulations have been reviewed to assess the applicability of current damage models, including the WRLM and Shakedown theory.

This paper presents the change in contact energy levels under different conditions in metro lines and a selected GB mainline route. In addition, the study used Shakedown theory to further investigate the damage propensity in LUL tracks and to evaluate the efficiency of Tγ for use in damage predictions.

London Underground (LUL) is the oldest and one of the busiest metro railway network in the world. The high traffic demand increases the average track tonnage to approximately 22 and 29 MGTPA (million gross tonnes per annum) for Bakerloo and Jubilee lines, respectively. Previous study which was undertaken at Vienna Underground stated that the track tonnage in metro lines were at the same range with conventional main railway lines. The track loading on Federal Austrian Railways was 23.36 MGTPA which is similar to the 18.96 MGTPA at Vienna Underground (Valenta et al. 2013). Therefore, it was concluded that the susceptibility of RCF cracking in rails did not depend solely on track tonnage, axle-load and speed; rail material, wheel profile and vehicle characteristics also play a key role.

Previous research focused on the RCF cracks in metro lines has highlighted some important findings. For instance, another study in Vienna Underground investigated the so-called as surface break-out type of defects which generally occur in curved track sections, but, in the case of Vienna Underground, these were located in curved track just before the stations. This is where the metro trains decelerated and hence the forces increased on the outer rail of the track (Fischmeister et al. 2009). Excessive tangential forces acting on the uppermost perlitic layer of the rail and followed the large plastic deformations in the surface was cited as the cause. They then merge with the subsurface damage which was already started to develop by the high normal loads caused from repetitive cycles.

Similarly, the study which analysed the RCF cracks in Attiko Metro in Athens through non-destructive evaluation and metallographic sectioning found that the larger number of cracks were observed in the curve sections as well as braking sections before the stations (Haidemenopoulos et al. 2006). It was noted that if the cracks tend to be not connected to each other on the surface, they often merge in the subsurface. These cracks had a depth of approx. 4 mm, but the crack subsurface lengths were varied between 20 and 50 mm stemming from the various crack initiation angles.

The earlier investigations conducted for LUL confirmed some of the aforementioned findings and suggested some of the critical points. It was revealed that the severity of the cracking substantially increased with the introduction of a new rolling stock. Therefore, a considerable level of effort was carried out to understand the current damage mechanisms on rails and wheels and to take precautions, particularly for the lines where new rolling stock (or upgrades to existing rolling stock, e.g. change in traction package) or a change in driving operation mode (from manual to automated systems) were planned to be introduced (Lewis and Olofsson, 2009).

In a separate study, one of the most prevailing type of rail defects, squats were analysed in detail on LUL (Grassie et al. 2011). Contrary to squat formation mechanism, these investigated defects were initiated by the limited wheelslip in poor adhesion areas, mostly approaching to signals on open track sections and resulted in thermal damage to the rails. In addition, large plastic flow which was often generated on the rail surface and pronounced to be a major factor in squat formation was not noticed in these defects since there was only minimal accumulated plastic flow took place around the crack mouth. Hence, a new name was given and called as studs (squat-type of defects).

2 Data analysis

2.1 Site description

In this study, the Bakerloo and Jubilee lines were selected in order to compare the rail damage mechanism in different operating conditions and to evaluate the effect of automatic train operation (ATO) on rail damage.

LUL carried approximately 1.5 billion passengers between the years 2014-2015 and the Bakerloo line was declared to be ninth busiest line in the network. The line has total distance of 23.2 km and there are 25 stations. It consists of both deep tube and surface sections. The geometry of the line includes sharp curves with a minimum

curve radius of 85 m. Check rails are installed on curves which have radius smaller than 200 m. The line is operated under manual mode with an average speed is approximately 50 km/h. In this study, the tunnel section between Elephant and Castle and Queen's Park is modelled using vehicle dynamics route simulations.

The Jubilee line is relatively longer than the Bakerloo line, 36.5 km, due to inclusion of Jubilee Line Extension (JLE) Project in 1999. This extension is passing through one of the crucial business centre of the city, London's Dockland Area and hence the number of passengers considerably increased and became the third busiest line in the LUL network. Nevertheless, it caused some part of the line are constructed with newer tunnels and low vibration track systems. In comparison to Bakerloo line, the Jubilee line is operated under automatic train operation (ATO) mode and the running speed reaches 90 km/h at several locations. It has also curvaceous track geometry, but the minimum curve radius is increased to 250 m. Therefore, checks rails are not required for this line. The actual cant value varies along the line, but due to increased running speeds, the cant deficiency raises in the line and reaches a maximum of 80-85 mm.

2.2 Defect data sheet analysis

LUL currently uses non-destructive testing (NDT) devices, such as ultrasonic and/or magnetic flux leakage based sensors, and carries out visual inspection to detect rail defects in tracks. To validate the outputs of NDT measurements and to estimate the potential risks, each rail defect is verified by visual inspection. The defects are recorded by an inspector in the rail defect form. This report includes the date of inspection, rail defect type, its severity, location, repair/maintenance technique and the minimum actions which have to be taken before its removal. These defect reports are listed in Defect Data Sheets which are prepared for each railway line on LUL. The defect data sheets for the Bakerloo and Jubilee lines were evaluated for the years 2013-2015 in order to identify the crack patterns observed in the rails.

Figure 1 shows the distribution of defects reported on the Bakerloo and Jubilee lines. The most predominant type of defect was squats, which is approximately 52% and 67% of the total defects on the lines. The results verified the findings of previous LUL study and demonstrated that they are not limited to conventional, high speed and freight lines but they are also frequently observed on the metro systems. Although squats were observed particularly on the shallower curves and tangents of open tracks sections on Jubilee line, they were reported on the sharper curves in the tunnel section of the Bakerloo line. When a squat type of defect has exceeded a certain value, it is recorded as Squat with T/O (Tache Ovale) which corresponds to Transverse defect from RCF in the Figure 1. The results indicated that approximately 25% and 10% of total squats recorded in the Bakerloo and Jubilee lines had a tendency to propagate further and increase the risk of a potential rail break.

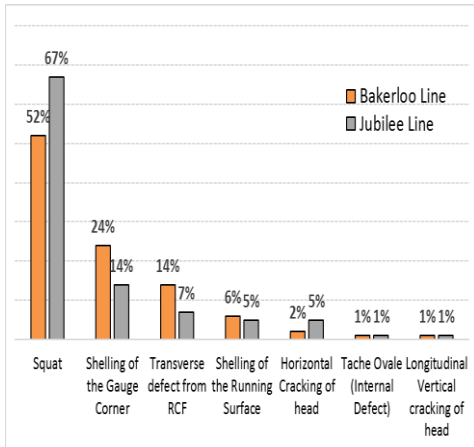

Figure 1: Reported defects on Bakerloo and Jubilee lines

The second prevalent type of defect was shelling which was recorded both on the gauge corner and top of running surface. The shelling type of defects are often initiated in the subsurface or near the surface. These initiated cracks then merge together and cause localised loss of structural integrity which results in shelling of the surface material. Therefore, the increased proportion of them showed that the metro systems are also generating excessive forces at the wheel-rail interface. On the contrary to squats, gauge corner shellings were mainly reported on the narrower curves of the old tunnel section in Jubilee line. Whereas the majority of them were recorded on the high rails, the low rails and tangent sections also seem to be susceptible

to this damage. Figure 2 and 3 show examples of shelling and squat type defects observed on the LUL tracks.

Figure 2: Example of a shelling defect observed on the LUL tracks

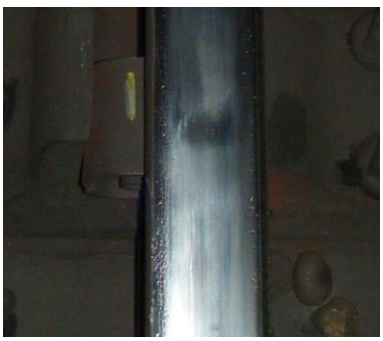

Figure 3: Example of a squat defect observed on the LUL tracks

In addition, the higher number of defects in the lubricated and open track sections potentially suggested the adverse effect of fluid on crack propagation which has been primarily investigated in the previous RCF crack growth modelling studies. One of the study which investigated this influence on crack growth rate found that fluid pressurization raised the crack growth especially for small cracks in 4-5 mm length (Fletcher et al. 2008).

Even though the previous metro system studies stated that the higher number of defects were observed on the braking sections before stations, the defect data analysis demonstrated that larger number of defects recorded in the traction areas, where the trains are accelerating out of the station platforms both on Bakerloo and Jubilee lines.

When the effect of ATO was evaluated, it was observed that a significantly greater number of defects were reported on the Jubilee line. This is also indicated in the inspection data with approximately 120 more shelling and 650 more squat defects recorded on the Jubilee lines between the specified dates. This suggests a potential influence of traction/braking forces on the resulting damage.

3 Prediction of rail damage

The phenomenon of RCF has been investigated for many years. Various models have been developed by applying different techniques and laboratory tests conducted to understand the reasons behind the problem. In reality, the complex nature of stress and strain fields of an RCF crack is under influence of many factors stemming from changing operational characteristics. Therefore, the parameters which are taken into account might sometimes not be sufficient to accurately model the observed damage. In addition, the Finite Element (FE) modelling technique which is often used in crack growth models is not appropriate to describe the significant variation in operating conditions observed in reality. As a consequence, a more pragmatic and quicker approach is needed to define the material's response to the applied forces and displacements.

3.1 WLRM damage function

In order to consider the real conditions of track and to make damage predictions in large railway networks, one of the well-known approaches is the Whole Life Rail Model (WLRM). This model provides an opportunity to investigate how different vehicle types, speeds, wheel and rail profiles and track geometries influence rail wear and RCF formation by integrating a large number of vehicle dynamics simulation outputs. The main input of the model is the wheel-rail contact patch energy ($T\gamma$).

It is calculated from the sum of the products of the creepage and creep forces

$$T\gamma = T_x\gamma_x + T_y\gamma_y + M_z\omega_z$$

Where; (Tx, Ty) and (γx, γy) are the tangential creep forces and the corresponding creepages in

the longitudinal and lateral directions respectively, and *Mz* and wz are the spin moment and the corresponding spin creepage respectively. It was assumed that this energy must be dissipated in some form, such as noise and/or heat, but it was argued that the majority of the energy would be released by wearing the wheel-rail contact surfaces (Allen, 1978) and (McEwen and Harvey, 1986).

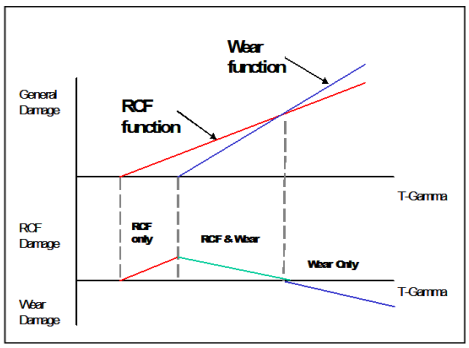

Figure 4: The combination of wear and RCF functions in the WLRM (Dembosky, 2004)

The model can account for the competition between wear and RCF by describing the regions where material removal through wear would be the dominant mechanism and the regions where RCF damage would be more likely to accumulate. Figure 4 shows the development of WLRM Damage Function from the separate RCF and Wear damage functions (Dembosky, 2004).

After several revisions, the WLRM took its final form shown in Figure 5 where the RCF Damage Function is divided into three regions. At low levels of energy, which is defined as the fatigue threshold (15 J/m (N)), the energy in the wheel-rail contact is insufficient to generate damage and therefore the predicted damage is zero. When the fatigue threshold is exceeded, the model shows positive RCF damage (referred to as RCF Only) which reaches a peak damage at 65 J/m (N). In the "RCF and Wear" region, the energy levels (> 65 J/m (N)) increase and wear begins to dominate but the wear is insufficient to remove the initiated cracks. When the Tγ values exceed 175 J/m (N), the predicted damage passes through zero to negative values. In this region, the wear rate dominates the cracks growth and the wear becomes sufficient to remove initiated cracks (Bevan, 2011).

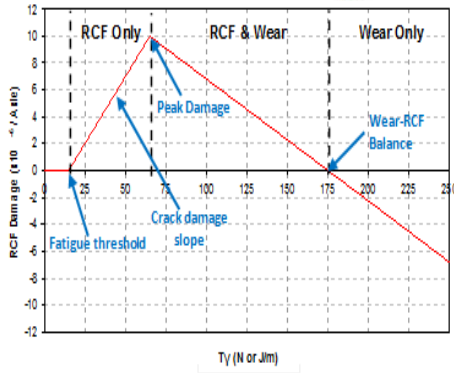

Figure 5: WLRM RCF damage function

The WLRM uses the "Signed Tγ" to predict rail damage. This assumes that the creep force in the traction directions leads to cracking in rails whereas, forces in the braking direction results in wheel damage. This assumption also supports the effect of fluid pressurization and entrapment mechanisms on crack growth in which the traction force at the wheel-rail contact moves over the crack and helps fluid inside the crack to apply pressure towards the crack tip (Burstow, 2006).

3.2 Vehicle dynamics route simulations

The Bakerloo and Jubilee line route simulations were performed using the Vampire vehicle dynamics software. The simulation cases include the effect of variations in track irregularity levels, applied lubrication and different wheel and rail profile combinations. An additional torque was also applied to the wheelsets to model the influence of traction/braking forces.

For comparison, a GB rail mainline route Midland mainline (MML) was also modelled in Vampire. The characteristics of this route are similar to those originally used to develop and validate the WLRM.

The primary difference between the selected routes is that MML includes mixed traffic whilst the LUL lines mainly operate with a single type of rolling stock. However, the track geometry, operating speeds and stop-start nature of metro systems also differs to main-line routes. Additionally, the track construction on metro systems influences the performance at the wheel-rail interface. For example; on LUL, several platforms are located in curve sections

especially on the Bakerloo line and check rails are installed on the curves with a radii of 200 m or less. Rail profile shape also varies frequently throughout the route, including the use of both bullhead (BS95lb) and flat-bottom (56E1) rail types. Furthermore, the lubrication strategy differs, with track–mounted lubricators mainly placed at the beginning of the critical curves. However, when these curves are located in platform regions the application point is moved as the low friction may influence the adhesion levels on the approach to stations and therefore increase the braking distance.

4 Simulation results

The influence of a number of factors on the Tγ output from the Vampire simulations has been investigated to test the applicability of WLRM for predicting rail damage on metro-underground systems.

4.1 Effect of curve radius on Tγ

The curve radius is one of the significant factors which influences the performance of the vehicle and therefore the predicted Tγ. Even though the minimum curve radius is often between 300-500 m range in mainlines, this range reduces to 100 m in metro lines. Figure 6 shows the distribution of curve radius on the selected routes. Bakerloo line consists of a large proportion of tighter curves between 100-150 m. Both lines also include a high proportion of curves in the 400-500 m radius range. The prevalent curve radius on MML is significantly greater, in the range 1500-1600 m.

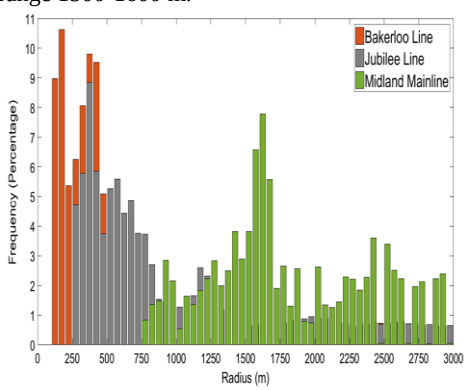

Figure 6: The curve distribution along the lines

As mentioned in the previous section, the WLRM uses the "Signed Tγ" assumption which is based on the fact that the angle-of-attack of wheelset in curved track modifies the direction of moment about the axle centre and it generally results in a positive longitudinal creep force on the high rail and a corresponding negative force on the low rail. The assumption proposed that this forward (positive) direction increases the risk of RCF damage on the high rail and wheel damage on the low rail. When the longitudinal creep force direction of each contact on tracks was analysed, it can be seen that the flange contact is usually in the traction direction rather than the tread contact on the high rail. Thereby, the previous WLRM studies have mostly taken into account the signed Tγ values at the wheel flange/gauge corner contacts at the outer wheel of the leading axle. For instance, the high contact energy (>=175 N) which is generated at this contact was defined to be responsible for the abrasive level of side wear in rails (Burstow et al. 2011).

However, the check rail contact in Bakerloo line restricts the level of wheel flange contact on the high rail. In addition, the high traction forces especially in the station areas might influence the direction of the creep force and make it positive for both low rail and tread contacts. Therefore, while flange contacts have lower energy in these curves (R<200 m) due to check rail contact, tread and low rail contacts have greater Tγ values, resulting in higher levels of predicted wear than RCF.

In order to demonstrate the different Tγ levels for each contact point, the predicted mean 'signed Tγ' was determined for each curve radius as presented in Figures 7 and 8. The former shows the mean 'signed Tγ' at the flange contacts and the latter gives the tread and low rail contact results for each line. Therefore, due to a change in the creep force direction, the mean "signed Tγ" values at flange contact on Bakerloo line were very small in checked curves (R<200m) but increase when check rails are not present (R>200m). This will result in less flange wear, but higher levels of predicted wear (rather than RCF, Tγ>175N) at the tread and low rail contacts.

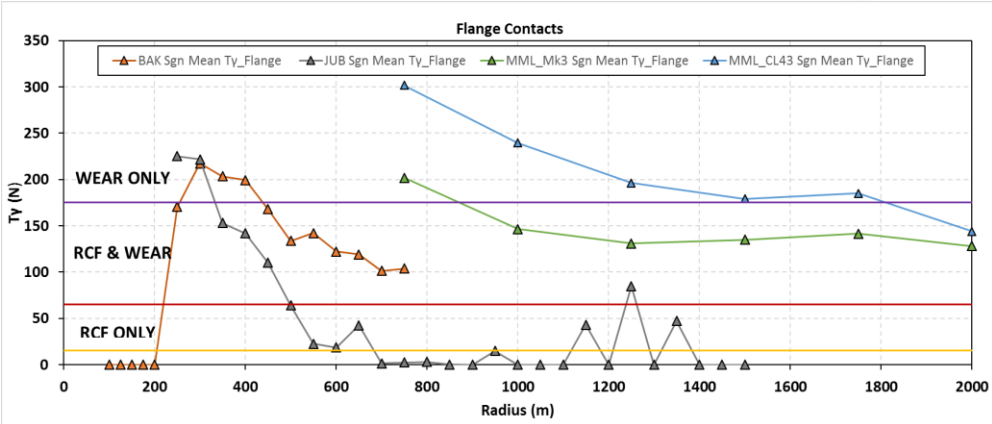

Figure 7: Effect of curve radius on mean 'signed Tγ' at Flange contact

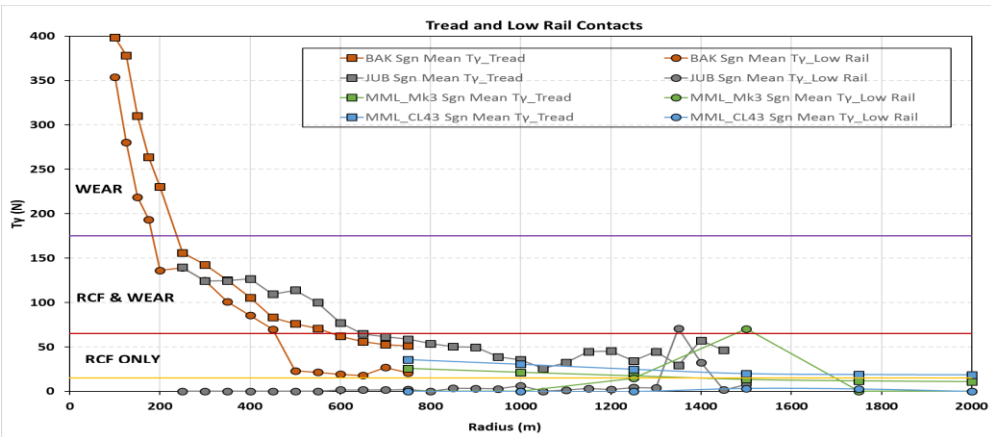

Figure 8: Effect of curve radius on mean 'signed Tγ' at tread and low rail contact

The Bakerloo and Jubilee lines generate similar results at curve radii of 300 m, with a "signed Tγ" of 220 N. But as the curve radius increases the flange contact produced higher results on the Bakerloo line. This might be a result of the different vehicle performance of 72 Tube Stock and effect of wheel profile utilised on this line.

On the MML, the Class 43 diesel locomotive and Mark 3 coach have been considered in this study. The heavier axle loads and increased running speeds result in higher mean "signed Tγ" values, particularly for the Class 43 locomotive.

As expected from previous WLRM results, the flange contacts produce higher 'signed Tγ' values and the wear was the most dominant damage mechanism especially on the sharper curves of mainline routes. The RCF risk became crucial for shallower curves. On the other hand, the tread contacts generally showed lower values and due to the negative creep force direction, the mean 'signed Tγ' values were generally 0 at low rail contacts. However, the creep force became positive between 1350-1600 m and increased RCF risk on these areas.

The infrastructure characteristics as well as the additional traction forces play a key role at the wheel-rail interface on metro tracks and influence the "signed Tγ". For example; the use of check rails raises the wear damage risk on both tread and low rail contacts, but reduces the damage risk at flange contacts. Again, on the contrary to mainline route, both the flange and tread contacts contribute to RCF damage risk on curves of both the Bakerloo and Jubilee lines.

Despite the good predictions of high rail RCF on mainline sites using the WLRM and 'signed Tγ' assumption, the defect data analysis demonstrated that both wear and RCF cracks were recorded on high side of checked curves and certain low rail sections on both of the metro lines. In these cases, the 'signed Tγ' assumption might reduce the accuracy in predicting the observed damage. It has been stated in previous WLRM studies that the use of 'signed Tγ' parameter gave considerably good validation particularly in respect to classic high rail RCF, but in certain circumstances it resulted in an over- or under-estimation. This was particularly evident on high rails of tighter curve radii and prediction of low rail damage. In order to increase the model's efficiency, it was suggested that different creep force angles may generate different types of damage and the subsequent studies showed the relationship between the resultant creep force angle and damage risk (Evans et al. 2008; Bevan, 2011). For this reason, the 'raw Tγ' and the creep force angle should be taken into account to improve the model's predictions.

Figures 7 and 8 illustrate the contact energies produced from the leading axle only. However, each axle pass, especially on mixed traffic routes where different type of vehicles are running on the tracks, result in various levels of wear and RCF damages. For example; several passages of a Mark 3 coach might contribute to RCF crack growth, whereas a single passage of a Class 43 may remove the initiated cracks. Therefore, the damage generated by each axle pass should be accumulated to account for interaction of wear and RCF for the life of the rail. Additionally, the variety of worn profiles in real traffic operations causes the contact patch to occupy a range of locations and influences wider regions on the railhead. For example, the worn wheel-rail profiles and the lateral shift of check rails change the contact positions over time and result in flange contacts which may be responsible for the gauge corner shelling in these sections. Therefore, an accurate damage prediction model should consider the aforementioned range of duty conditions observed by the rail and to reflect these variations in its model output.

4.2 Effect of friction on Tγ

The WLRM uses a wheel-rail coefficient of friction of μ=0.45 (Bevan, 2011). This was primarily due to the uncertainty in the actual friction conditions on track and to incorporate the worst case scenario into the model. However, in reality friction conditions vary due to changes in weather, environmental conditions and lubrication regime. LUL utilises several different kinds of lubrication systems, such as vehicle and track mounted lubricators, in order to prevent wear and reduce noise. Information on the position and the type of lubricator was obtained from LUL and a track parameter file was used in the Vampire to vary the friction level along the track.

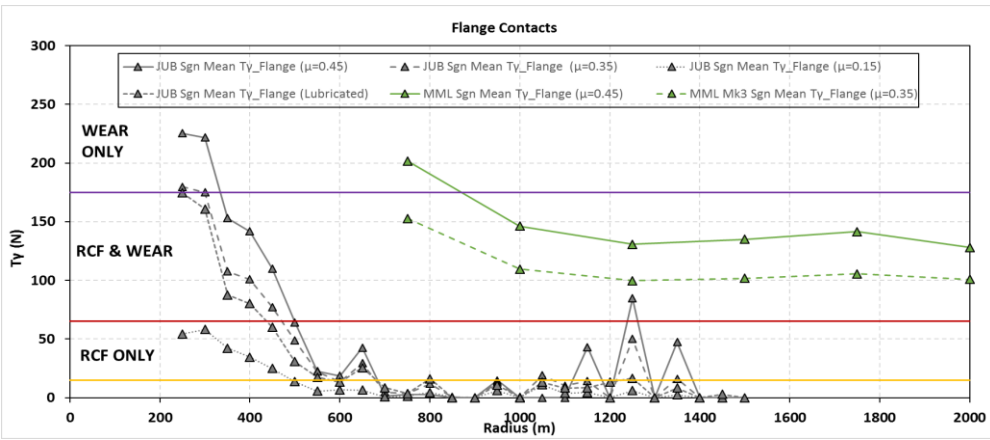

Figure 9: Effect of different friction conditions on mean 'signed Tγ' at flange contact

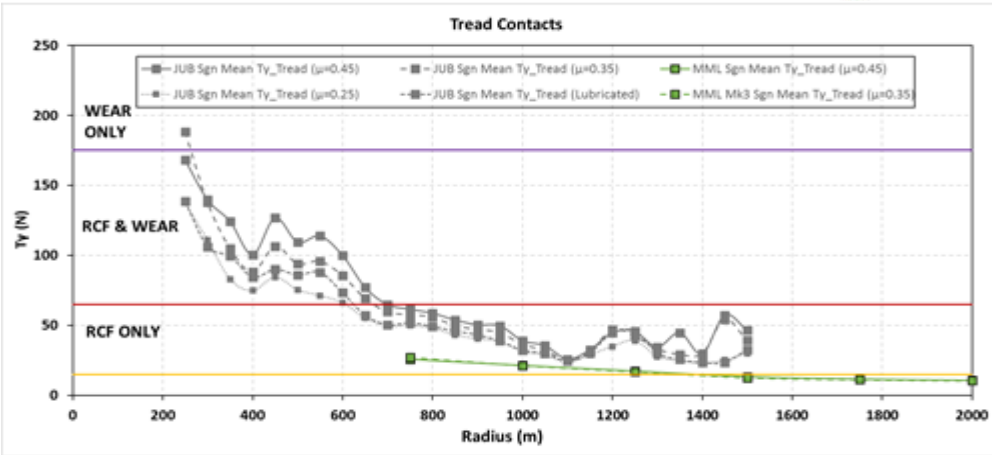

Figure 10: Effect of different friction conditions on mean 'signed Tγ' at tread contacts

To demonstrate the influence of friction on Tγ, the route simulations were conducted by using different friction coefficients. As the lubrication is usually applied on high rails, the mean 'signed Tγ' values were only compared for flange and tread contacts which are shown in Figures 9 and 10 respectively.

The lower friction coefficients resulted in lower Tγ values at both contacts. The major impact was observed at the flange contact with a reduction in Tγ from 225 N to 175 N on the 250 m radius curve. Similar to the Jubilee Line, the Tγ values at the flange contact on the MML were reduced by 50 N with a friction coefficient of μ=0.35. On the other hand, the results at the tread contact in this line did not show a significant change due to lower creepage values at this contact. The lubrication estimation in the model produced relatively smaller values when the friction coefficient remained in the μ = 0.25 - 0.35 range. However, although lubrication condition reduced the Tγ at the wheel-rail contact, interaction of wear/RCF may raise the crack growth rate and make the high rails more susceptible to RCF damage risk which was also observed in the field defect data analysis.

4.3 Effect of track irregularity on Tγ

The installation errors during the track construction stage and the deviations caused by high number of vehicle passages lead to track irregularities in the railway lines.

The Track Recording Vehicles (TRV) measure the track alignment in certain intervals and collect information such as curvature, vertical and lateral irregularities, cant and gauge variations.

Figures 11 and 12 compare the influence of track irregularities on the mean 'signed Tγ' at the flange and tread contact respectively. Removing (No IRR) and scaling (Sc IRR) the track irregularities did not seem to influence the mean Tγ values on Jubilee line, but they influence the distribution of the contact position on the railhead. For example, there was no flange contact generated with zero and scaled irregularities at shallower curve radii, whereas with irregularities flange contact occurred on 1250 m radius with a mean 'signed Tγ' of 85 N. In comparison to Jubilee line, the mean 'signed Tγ' at flange contact on the MML was significantly reduced with zero track irregularities. While the ballasted track on MML might have a greater impact on track irregularities, the slab track on the majority of Jubilee line may have a lesser influence. However, the Tγ was not affected at tread contacts of both of the lines. Therefore, while track irregularities have relatively small effect on the mean 'signed Tγ' results presented in the Figure 11 and 12, larger variations were observed on the contact positions. This means that a larger proportion of the railhead is susceptible to damage and shows the importance of accumulating damage across the railhead to account for these variations.

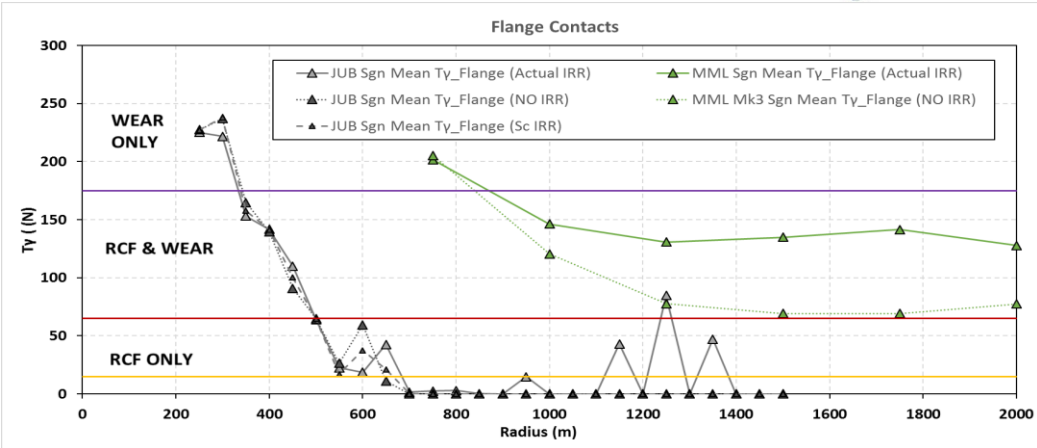

Figure 11: Effect of track irregularity on mean 'signed Tγ' at flange contacts
(Note: Actual IRR = measured TRV data, No IRR = No irregularities and Sc IRR = Scaled irregularities)

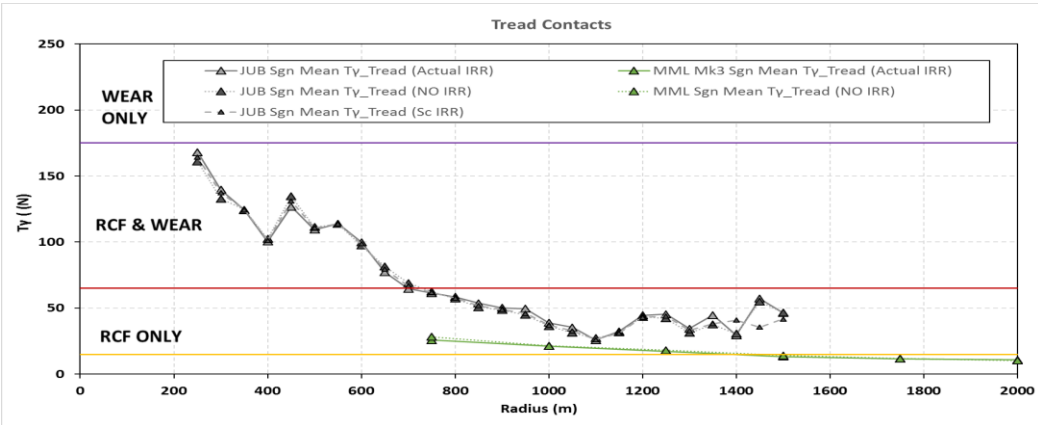

Figure 12: Effect of track irregularity on mean 'signed Tγ' at tread contacts
(Note: Actual IRR = measured TRV data, No IRR = No irregularities and Sc IRR = Scaled irregularities)

4.4 Effect of different wheel-rail profile combinations on Tγ

In the rail damage modelling, it is important to take into account for different wheel-rail profile combinations. The wheel and rail geometry play an important role in the determination of contact conditions. The results provided in the previous figures were prepared considering new rail and wheel profile pairs. However, the shape of rail profile can change frequently along the route due to wear, grinding and/or renewals. Similarly, the wheel profiles are also worn over time and reprofiled at different intervals.

Figures 13 and 14 present the influence of the worn profiles on the predicted mean 'signed Tγ' at the flange and tread contacts respectively. Generally, wheel and rail profiles wear to shapes that give rise to conformal contacts at the wheel-rail interface, resulting in an increase in conicity. In the case of the Jubilee line, the selected worn profile combinations generate a lower conicity than the new case, resulting in a reduction in the Tγ at the tread contact and an increase at the flange contact. This means that severe flange wear would occur in wider range of curve radii, whereas the reduction in Tγ on the tread potentially increases the 'RCF Only' damage risk. Conversely, the worn profile combinations used in MML simulations lead to an increase in conicity, reducing the level of flange contact and 'signed Tγ' but an increase in Tγ can be seen at the tread contact. This

potentially reduces the level of RCF susceptibility at flange contacts but increases at tread contacts. It was also noted that the worn case in MML did not produce any flange contacts on 750 m and 1750 m radius curves.

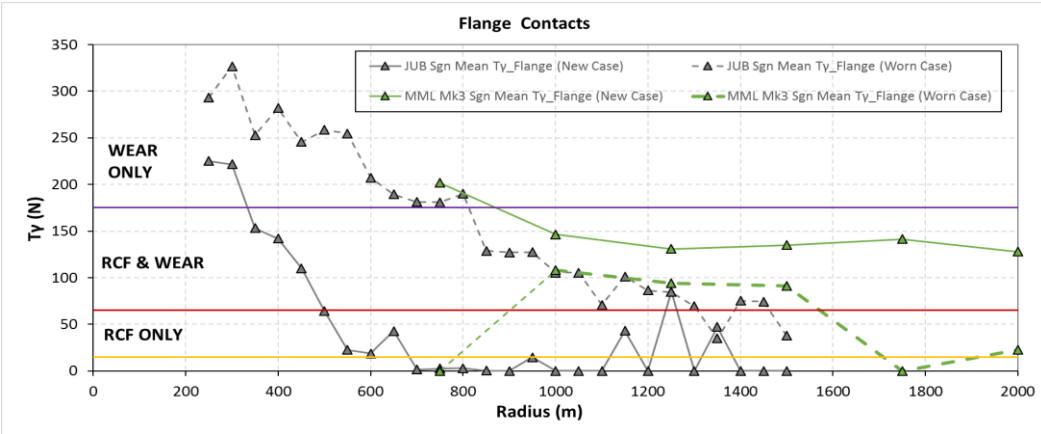

Figure 12: Effect of worn case on mean 'signed Tγ ' at flange contact

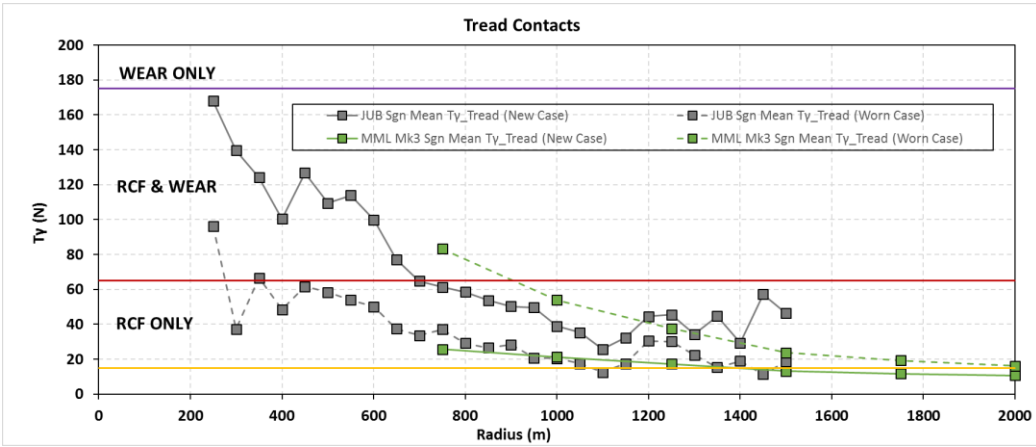

Figure 13: Effect of worn case on mean 'signed Tγ ' at tread contact

5 The relationship between *Tγ* and Shakedown diagram

One of the significant approaches used in assessing the propensity of a rail material to RCF cracking is the Shakedown theory (Johnson, 2000). This can be represented as a Shakedown diagram as shown in Figure 15, which illustrates the materials' response under different combinations of normal and shear loads within the contact patch. If the stresses produced in the wheel-rail contact are below the elastic limit given in the Shakedown diagram, then it was found that no permanent deformation will occur. However, in the real condition, these stresses mostly exceed the elastic limit and cause plastic flow near the surface. Although the residual stresses are developed in the rail head which increase the resistance of the rail to cracking, the high number of passages combined with heavy axle loads will result in an exceedance of shakedown limit. If the maximum load for shakedown is again exceeded, then permanent plastic deformation will generate in the material. With each cycle of load, the plastic deformation will accumulate by the process called ratchetting which is also known as "incremental collapse" (Ponter et al. 1985). The shakedown diagram

uses the parameters: load factor (Po/k) and traction coefficient (f) which is given in Figure 15. When the applied load is lower than the elastic shakedown limit, failure will occur eventually by high cycle fatigue which means that a high number of cycles are required for failure to take place in the material. Above this limit, plastic deformation is generated by each cycle and the material fails by low cycle fatigue. However; when the plastic shakedown is exceeded, ratchetting failure occurs and the material becomes unable to sustain any further plastic deformation (Franklin et al. 2003). It was suggested in the related study that the occurrence of failure in rails is generated by either low cycle fatigue or ratchetting failure mechanism leads to the shortest life in rails.

The load factor and traction coefficient is calculated as follows:

$$P_0/k = \frac{3F_N}{2\pi abk} \qquad f = F_T/F_N$$

where P_0, is the maximum contact pressure (MPa), k (K_e) is the shear yield strength of the material (MPa), F_T is the tangential force (N), F_N is the normal load (N) and a, b are the semi-axes of the wheel-rail contact patch.

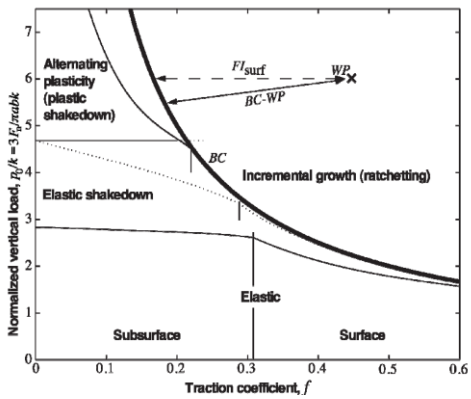

Figure 15: Shakedown diagram

In the previous sections, the mean 'signed Tγ' results were plotted for the range of curve radius on the lines. It was demonstrated that this parameter was able to reflect the influence of changes in operating conditions on the susceptibility to rail damage. In addition, when the values were compared with the damage locations on the studied lines, it provided relatively good agreement with the field data in particularly low rail of checked curves and high rail of curved sections. However, the results were not satisfactory especially in tangent and low rails of R>200 m curved tracks. In order to further evaluate the model's efficiency, changes in Tγ, its relationship with Shakedown diagram was investigated in the study. Both the mean 'raw Tγ' and 'signed Tγ' values with their corresponding mean load factor and traction coefficient were taken into account to identify the differences between these two parameters and to find the most influential variable on the Shakedown theory.

Figures 16 and 17 present a comparison of the load factor, traction coefficient and corresponding 'raw Tγ' and 'signed Tγ', values at the flange contacts for the three lines studied. In these figures, the colour of the points represents the line, whereas the shape of the marker represents the Tγ range. As it can be seen in the figures, there is a correlation between the Shakedown parameters and Tγ for each of the lines. The higher values of Tγ (>175N), which were mainly associated with the wear, generate the highest load factors for each line. Although higher axle loads are apparent on the MML, the smaller flange contact patch area raised the contact pressure values on sharper curves of Bakerloo line resulting in the highest load factors. In this case, the majority of the flange contacts exceeded the shakedown limit on both Bakerloo and MML. However, only the sharper curves (250-300m radius) with possible wear risk on Jubilee line exceed this limit. The shallower curves, especially between 500 m and 1500 m radius, were shown to generate a very low damage risk (since they appear below the elastic shakedown limit, as highlighted in Figure 16), possibly as a result of the characteristics of the wheel profile used on this line. The positive creep force direction in 'signed Tγ' resulted in a similar mean traction coefficient for a range of curve radius considered in the study.

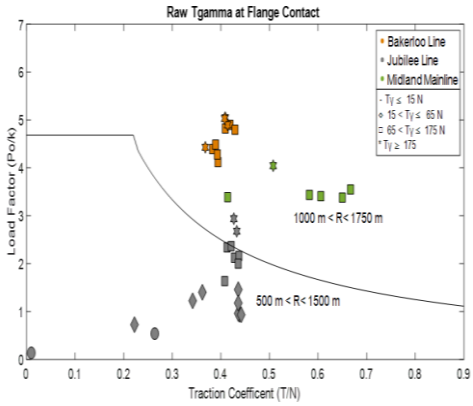

Figure 16: The relationship between 'raw Tγ ' and shakedown diagram at flange contact

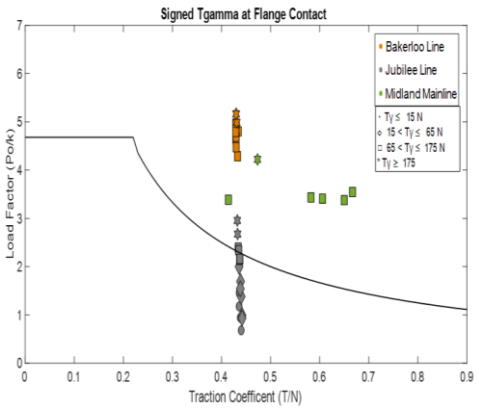

Figure 17: The relationship between 'signed Tγ' and shakedown diagram at flange contact

The tread contacts produced relatively mixed results compared to flange contacts which are shown in Figures 18 and 19. Even though the Tγ values were extremely high on checked curves, the larger contact patch area of the single tread contacts reduced the contact pressure in these sections. However, the normal load at tread contact of two-point contact cases became more critical and created larger load factors compared to the flange contacts. For instance, the aforementioned drop in the severity of flange contacts lead to excessive damage risk at tread contacts on Jubilee line. In addition, the shakedown diagram demonstrated that the non-fatigue (Tγ≤15N) regions in MML are very close to limit and might also cause RCF in rails.

In contrast to flange contacts, there was no significant different observed between mean 'raw' and 'signed Tγ' values at the tread contacts. But, the signed criterion significantly decreased the number of contacts considered in the analysis. Whereas some of the mean 'signed Tγ' values were reduced such as the wear risk 'raw Tγ' was shifted to the RCF region 'signed Tγ' in Jubilee line, the load factors substantially increased in Bakerloo line.

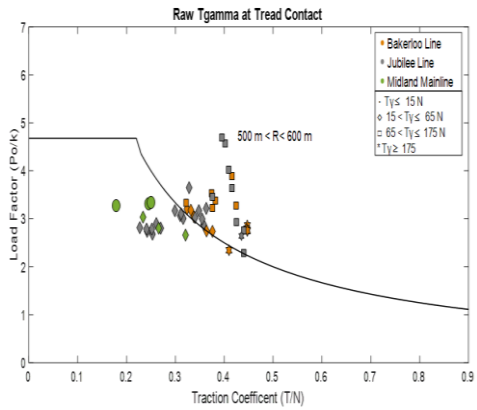

Figure 18: The relationship between 'raw Tγ ' and shakedown diagram at tread contact

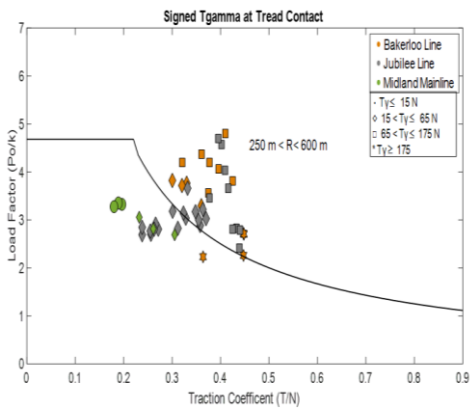

Figure 19: The relationship between 'signed Tγ ' and shakedown diagram at tread contact

The shakedown diagrams which are presented in Figures 20 and 21 clearly pointed out the differences between the Tγ parameter and shakedown diagram since, the considerably lower energy values on MML generated the highest risk levels displayed in the shakedown

diagram. Whereas the heavy axle loads were often distributed between flange and tread contacts and caused moderate contact stresses on high rails, the larger normal loads at the single low rail contact makes these rails more vulnerable to damage than the metro tracks. The Figures also illustrate the difference between the 'raw Tγ' and 'signed Tγ' values especially on LUL tracks. Although, the 'signed Tγ' suggested that only the curves between 100-400 m radius were under higher risk levels and showed that the majority of these contacts might cause RCF risk, the results could not exceed elastic shakedown limit. However, the 'raw Tγ' values demonstrated that these rails might also cause RCF cracks either by low cycle fatigue or ratchetting mechanism.

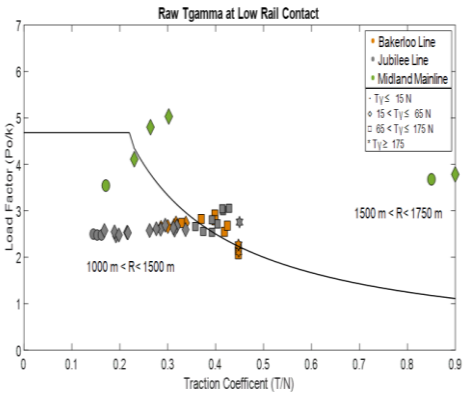

Figure 20: The relationship between 'raw Tγ ' and shakedown diagram at low rail contact

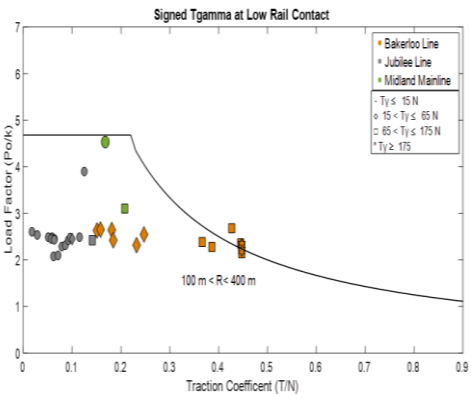

Figure 21: The relationship between 'signed Tγ' and shakedown diagram at low rail contact

The shakedown diagram provides useful results to understand the material's response to the applied forces. It showed that the high rails (both flange and tread contacts) were to a greater extent susceptible to RCF cracking. However, in contradiction to expectations that heavier axle loads lead to higher contact stresses, in some cases the metro systems caused larger load factors.

As it can be seen from these figures, there is a clear relationship between the Tγ and shakedown parameters especially the traction coefficient. But, this approach also showed that some contacts with $T\gamma \leq 15$ N were potentially susceptible to damage. For example, while the WLRM predicted damage on low rails of only Bakerloo line, both the 'raw Tγ' and shakedown criterion demonstrated their severity in other lines. In addition, the treads contacts with no RCF risk on MML shown to be susceptible to damage risk under low cycle fatigue mechanism. Moreover, when the 'raw' and 'signed Tγ' values were compared in detail, it was noticed that the positive creep force direction definitely reduced the number of contacts considered in the analysis.

Even though the shakedown diagrams seem to be appropriate in showing the damage propensity in rails, they demonstrated that the majority of the curves studied in the lines were under risk of RCF by either ratchetting or low cycle fatigue mechanism. However, the field crack data analysis indicated that no cracks were reported in some of the curved sections along the lines. The use of 'signed Tγ' was shown to eliminate some of the Shakedown exceeding values, but the previous studies suggested and the damage predictions confirmed that the assumption may underestimate some of the critical regions on the lines.

6 Conclusion and Future work

In this study, the susceptibility to rail damage was investigated using vehicle dynamics simulation on two London Underground (LUL) lines. Bakerloo and Jubilee lines were selected to evaluate the effect of different operating conditions on rail damage predictions. The outputs from the vehicle dynamic simulations were compared to a GB mainline route which

exhibits operating conditions similar to those used to validate previous rail damage predictions using the WLRM. These comparisons were performed to investigate the applicability of the WLRM, which has previously been validated on mixed traffic mainlines in GB, for use on metro-underground systems.

Firstly, LUL defect data sheets were analysed to understand the distribution and severity of reported rail damage on the studied lines.

Secondly, the outputs from detailed Vampire vehicle dynamic route simulations were investigated to review the susceptibility to rail damage on the selected lines, using the energy in the contact patch (Tγ) as an indicator. The Vampire outputs from each line were post-processed to investigate the influence of certain parameters (including: curve radius, friction coefficient, track irregularities, wheel/rail profiles) on the resulting 'signed' Tγ. The main observations from these simulations included:

- Curve radius; As the curve radius decreases on all the lines, the mean 'signed Tγ' values increased at all the contacts. Similar to previous WLRM studies, the smaller curve radius in metro tracks inevitably raised the Tγ at the flange contacts, but the heavier axle loads and the higher running speeds on MML had a significant impact on contact energy levels and increased the results substantially. However, the use of check rails (for curves with R< 200 m) on Bakerloo line as well as the additional traction forces in the stop-start nature of the metro lines influences the level of Tγ, resulting in the tread and low rail contacts being more susceptible to damage.
- Friction coefficient; Reducing the friction coefficient generally decreases the level of Tγ. However, although the lubrication condition decreased the wear risk, the increased RCF damage risk predicted by the WLRM might give rise to increased damage, as observed in the analysis of the field crack data.
- Track irregularities; The results showed that track irregularities did not significantly influence the predicted Tγ especially tread contacts, but they did influence the location of contacts on the railhead resulting in an increase in Tγ and RCF risk at flange contact, especially in shallower curves on both lines.
- New and worn wheel/rail profiles; The selected worn wheel/rail profiles for Jubilee line generated a lower conicty, reducing the Tγ at the tread contact, but increasing the levels at the high flange contact potentially resulting in increased susceptibility to wear. Conversely, the worn profiles combinations used in the MML simulations lead to a higher conicity resulting in less flange contact and an increase in Tγ and RCF risk at the tread contacts.

Finally, the relationship between the Tγ and the shakedown diagram was investigated. The comparisons included in the paper showed a good correlation between Tγ and susceptibility to generate damage on the high rail flange contact based on the shakedown criterion. Whilst on the tread and particularly low rail contacts, the shakedown criteria seemed to provide a better prediction of the curves more susceptible to damage. In addition, by predicting the level of failure mechanism, it highlighted the significance of RCF cracking in metro systems, as despite the relatively lighter axle loads, the sharper curves and smaller contact areas result in increased load factors when compared to conventional mainline.

The results from both the shakedown diagram and contact energy parameter have been shown to predict areas at risk to damage in several sections. However, in order to reduce the risks associated with under- (unplanned maintenance and renewals, increased maintenance costs) and over-estimation (premature rail replacements, lack of confidence in modelling) of rail damage, an accurate prediction of the severity and rate of damage is required. To achieve this, the modelling should consider the range of duty conditions observed by the rail from the successive vehicle passes. This should include the range of wheel and rail profiles, vehicle speeds, traction/braking forces and track irregularities.

References

Allen,P.A. (1978). An Hypothesis for the Prediction of Wheel and Rail Wear. (IM-DA-291). UK: British Railways Board.

Bevan, A. 2011. Further Development of the WLRM Damage Parameter: Integration

Report. T775-01 project report, Rail Safety and Standards Board (RSSB).

Burstow, M. (2006). Background to the Tγ RCF damage function, Network Rail.

Burstow, M., Dembosky, M., Gurule, S., Urban, C., (2008), Recent findings in the understanding of vehicle/track interaction on track damage and rolling contact fatigue RCF, UIC repository.

Dembosky, M. (2004). RCF in the UK system-the emerging solution. Paper presented at the Permanent Way Institution Journal and Report of Proceedings.

Evans, J., Lee, T., and Hon, C. (2008). Optimising the wheel/rail interface on a modern urban rail system. Vehicle System Dynamics, 46(S1), 119-127.

Fischmeister, E., Rossmanith, H., Loibnegger, F., Linsbauer, H., Mittermayr, P., and Oberhauser, A. (2009). From rail surface cracks to rail breaks–Recent investigations and results of research at the Wiener-Linien Metro System, 8th International Conference on Contact Mechanics and Wear of Rail/Wheel Systems (CM2009). Florence, Italy.

Fletcher, D., Hyde, P., and Kapoor, A. (2008). Modelling and full-scale trials to investigate fluid pressurisation of rolling contact fatigue cracks. Wear, 265(9), 1317-1324.

Franlin, F. J., Chung, T., and Kapoor, A. (2003) Ratchetting and faigue-led wear in rail-wheel contact. Fatigue & Fracture of Engineering Materials & Structures, 26.10(2003):949-955.

Girsch, G., and Heyder, R. (2003). Testing of HSH-Rails in high speed tracks to minimise rail damage. Paper presented at the Proceedings of the Sixth International Conference on Contact Mechanics and Wear of Wheel/Rail Systems (CM2003), Sweden.

Grassie, S. L., Fletcher, D. I., Hernandez, E. G., and Summers, P. (2011). Studs: a squat-type defect in rails. Proceedings of the Institution of Mechanical Engineers, Part F: Journal of Rail and Rapid Transit.

Haidemenopoulos, G., Zervaki, A., Terezakis, P., Tzanis, J., Giannakopoulos, A., and Kotouzas, M. (2006). Investigation of RCF cracks in a grade 900A rail steel of a metro track. Fatigue & Fracture of Engineering Materials & Structures, 29(11), 887-900.

Johnson, K. (2000). Plastic deformation in rolling contact: Springer.

Lewis, R., & Olofsson, U. (2009). Wheel-rail interface handbook: Elsevier.

Li, Z., Zhao, X., Esveld, C., Dollevoet, R., & Molodova, M. (2008). An investigation into the causes of squats—Correlation analysis and numerical modeling. Wear, 265(9), 1349-1355.

McEven I.J. and Harvey, R.F (1986). Interpretation of Wheel/Rail Wear Numbers. (TM-VDY-004). UK:.British Railways Board

Olofsson, U., & Nilsson, R. (2002). Surface cracks and wear of rail: A full-scale test on a commuter train track. Proceedings of the Institution of Mechanical Engineers, Part F: Journal of Rail and Rapid Transit, 216(4), 249-264.

Ponter, A., Hearle, A., and Johnson, K. (1985). Application of the kinematical shakedown theorem to rolling

Valenta, G., Varga, T., & Loibnegger, F. (2013). Investigations of rail fractures at vienna underground and measures to reduce them. Presented at the ECF13, San Sebastian 2000.

Vickerstaff, A. (2015). Predict and Prevent:The future of wheelset management on London Underground presented at the 21 Wheel-Rail Interaction Conference-Derby, UK.

Vickerstaff, A. (2016). A Holistic approach to WRI Management on London Underground at the 22 Wheel-Rail Interaction Conference-Las Vegas, USA.

Watson, A.S. (2002). Whole Life Rail Model: Initial Investigations into Traffic Pattern Effects, AEATR-T&S-2002-038, Issue 1, RSSB.